Journal of the European Ceramic Society **17** (1997) 689–696

PII: S0955-2219(96)00085-4
0955-2219/97/$17.00

Discrimination of Multiaxiality Criteria with the Brazilian Disc Test

A. Brückner-Foit,[a] T. Fett,[b] D. Munz[a] & K. Schirmer[a]

[a]Karlsruhe University, Institute of Reliability and Failure Analysis, PO Box 36 40, D-76021 Karlsruhe, Germany
[b]Research Centre Karlsruhe, IMF-II, PO Box 36 40, D-76021 Karlsruhe, Germany

(Received 20 November 1995; revised version received 18 April 1996; accepted 3 May 1996)

Abstract

A fixture was developed which allows us to test circular discs of high strength ceramic materials under diametral compression. This so-called Brazilian disc test can be used to determine the failure behaviour of natural flaws contained in ceramic materials under multiaxial loading, as a stress state with both negative and positive principal stresses is induced in a disc during the test. The results of the test series performed with low and high strength ceramics are analysed using the multiaxial Weibull theory. Comparison of the Weibull distributions of the fracture stresses obtained with the Brazilian disc test and the outcome of the other test series clearly shows that a shear-insensitive failure criterion is more suitable to determine the critical flaw size under mixed mode loading than a shear-sensitive criterion. © *1997 Elsevier Science Limited. All rights reserved.*

Introduction

The fracture behaviour of ceramics subjected to a multiaxial stress state can be predicted from uniaxial test data on the basis of the multiaxial Weibull theory.[1–3] In this theory the components of the stress tensor are expressed in terms of an equivalent stress which is determined on the basis of a fracture mechanics model. The natural flaws are assumed to be planar cracks of random orientation. The multiaxial stress field causes mixed-mode loading of these cracks, and the severity of loading can be expressed in terms of the corresponding mixed-mode stress intensity factor.

There are various criteria for evaluating failure under mixed-mode loading. Some of them are based on continuum mechanics criteria,[4–6] others are determined by careful evaluation of fracture mechanics test data obtained with steel specimens.[7] All these criteria are, strictly speaking, only applicable to well-defined planar cracks. It is not self-evident in advance which of these relations is the correct one for a specific ceramic material which, in general, contains three-dimensional flaws of very complicated shapes. Suitable test procedures have to be designed which will help to select the appropriate formula for the equivalent stress.

It can be shown by a straightforward calculation that the differences between the failure probabilities predicted by each of these criteria are comparatively small if only stress states with positive principal stresses are considered. Moreover, the inherent statistical uncertainties of test data are of the same order of magnitude for the sample sizes typically used in mechanical testing of ceramics. An example is given in Ref. 8, where results obtained with the four-point bend test are compared with those obtained with the concentric-ring test. However, there might be considerable differences in the predicted failure behaviour for stress states with both negative and positive principal stresses.

The Brazilian disc test,[9] in which a circular disc is subjected to diametral compression, was originally designed to determine the mechanical properties of concrete or rock materials. The loading induces a rather complicated biaxial stress state with $\sigma_1 > 0$, $\sigma_2 < 0$ or $\sigma_1 < 0$, $\sigma_2 < 0$, depending on the location in the disc.[10,11] Hence, the test is a good tool for determining the failure behaviour of ceramics under multiaxial loading. Apart from applications in rock mechanics, the test was successfully used only with low-strength ceramics.[12–14] Preliminary tests with high-strength materials showed that failure initiated from damage zones in the vicinity of the load pin. Hence, the measured value of the fracture strength depended mainly on the quality of the fixture.[15]

In this paper results obtained in the Brazilian disc test for high-strength ceramics are presented and analysed using the multiaxial Weibull theory, a summary of which is given in the first section. The experiments are described in the second section.

The third section contains the Weibull analysis of the results and a discussion of the experimental findings based on the multiaxial Weibull theory.

Theory

The failure of ceramics is triggered by unstable extension of natural flaws such as inclusions, pores, damaged grain boundaries, etc. These flaws are assumed to be of random sizes with random orientations and are randomly distributed in the material. The worst flaw determines the maximum tolerable load. A mathematical description of this behaviour can be given in terms of the extreme value theory,[16] leading to a Weibull distribution of the strength of ceramic materials. The failure probability of a component of volume V is given by:[1-3]

$$P_f = 1 - \exp\left[-\frac{1}{V_0} \cdot \frac{1}{4\pi} \int_V \int_\Omega \left(\frac{\sigma_{eq}}{\sigma_0}\right)^m d\Omega \, dV \right] \quad (1)$$

where m, σ_0 are material parameters, Ω is the unit sphere and σ_{eq} is the equivalent stress which, in turn, depends on the stress tensor $\sigma_{ij}(\vec{x})$ at the location $\vec{x}$ and on the orientation of the flaw plane. At a specific load level characterized by the reference stress σ^*, the stress tensor can be written as:

$$\sigma_{ij} = \sigma^* \cdot h_{ij}(\vec{x}) \quad (2)$$

where h_{ij} depends only on the geometry. The failure probability, eqn (1), can be re-formulated in terms of a Weibull distribution:

$$P_f(\sigma^*) = 1 - \exp\left[-\left(\frac{\sigma^*}{b}\right)^m \right] \quad (3)$$

with parameters m and b, where b depends on the stress distribution:

$$b = \sigma_0 \left[\frac{1}{V_0} \cdot \frac{1}{4\pi} \int_V \int_\Omega \left(\frac{\sigma_{eq}}{\sigma^*}\right)^m d\Omega \, dV \right]^{-1/m} \quad (4)$$

Any failure criterion for multimodal failure can be written in the form

$$g(K_I, K_{II}, K_{III}) \geq g_c \quad (5)$$

where g_c is a critical value characterizing the material resistance to unstable crack propagation; obviously, g_c is a function of the fracture toughness K_{IC} and possibly of K_{IIc} and K_{IIIc}. The equivalent mode I stress intensity factor, K_{eq}, is defined by the relation

$$g(K_{eq}, 0, 0) = g(K_I, K_{II}, K_{III}) \quad (6)$$

and the corresponding equivalent stress σ_{eq} follows from

$$K_{eq} = Y_I \sqrt{\pi a} \cdot \sigma_{eq} \quad (7)$$

where Y_I is the fracture mechanics correction factor for mode I loading.

The following failure criteria are considered in this paper:

(1) Mode I failure

$$g(K_I, K_{II}, K_{III}) = K_I \quad (8a)$$

$$g_c = K_{Ic} \quad (8b)$$

(2) Coplanar energy release rate[4]

$$g(K_I, K_{II}, K_{III}) = \frac{1}{E'}\left(K_I^2 + K_{II}^2 + \frac{1}{1-\nu} K_{III}^2 \right) \quad (9a)$$

$$g_c = \frac{K_{Ic}^2}{E'} \quad (9b)$$

where

$$E' = E \quad \text{(for plane stress)} \quad (10a)$$

$$E' = \frac{E}{1-\nu} \quad \text{(for plane strain)} \quad (10b)$$

(3) Maximum hoop stress factor[5]

$$g = \frac{\sqrt{8}(2K_I + 6\sqrt{K_I^2 + 8K_{II}^2}) \cdot K_{II}^3}{(K_I^2 + 12\,K_{II}^2 - K_I\sqrt{K_I^2 + 8K_{II}^2})^{1.5}} \quad (11a)$$

$$g_c = K_{Ic} \quad (11b)$$

(4) Maximum noncoplanar energy release rate[6]

$$g = \frac{1}{E'} \sqrt{K_I^4 + 6K_I^2 K_{II}^2 + K_{II}^4} \quad (12a)$$

$$g_c = \frac{K_{Ic}^2}{E'} \quad (12b)$$

(5) Empirical criterion of Richard[7]

$$g = \frac{1}{2}(K_I + \sqrt{K_I^2 + 4(c \cdot K_{II})^2}) \quad (13a)$$

$$g_c = K_{Ic} \quad (13b)$$

where c is an empirical constant.

The Weibull parameter b, eqn (4), depends on the stress field and hence on the loading and geometry of the specimen. The Weibull parameters of two different specimens are related by:

$$\frac{b_1}{b_2} = \left(\frac{H_2}{H_1}\right)^{1/m} \quad \text{and} \quad m_1 = m_2 = m \quad (14)$$

with

$$H = \frac{1}{V_0} \cdot \frac{1}{4\pi} \int_V \int_\Omega \left(\frac{\sigma_{eq}}{\sigma^*}\right)^m d\Omega \, dV \quad (15)$$

Different values of H, and hence of the ratio eqn (14), are obtained for different relations selected for the calculation of the equivalent stress. The

predictions of eqn (14) can be compared with the empirical distribution of the fracture stress in order to identify suitable multiaxiality criteria.

Experiments

Specimens of four different materials were subjected to uniaxial and multiaxial stress fields. The basic material properties are summarized in Table 1. The specimen geometries and test conditions are contained in Table 2. The results of the four-point bend test were used as reference samples for both the stoneware material and the alumina. No suitable uniaxial test data were available for the silicon nitride materials. A biaxial stress state with $\sigma_1 > 0$, $\sigma_2 > 0$ is induced in the concentric-ring test and the cold-spin disc test, whereas positive as well as negative principal stresses are present in the Brazilian disc test.

Table 1. Material properties

Material	*Young's modulus (GPa)*	*Poisson's (ratio)*	*Fracture toughness (MPa $m^{0.5}$)*
Stoneware (Keramische Betriebe Buchtal)	50	0·25	0·9
Al_2O_3 (CERASIV)	370	0·23	3
HIPSN (ABB)	310	0·24	4·3
HIPSN (ESK)	310	0·24	4·6

A standard fixture was used in the four-point bend tests.[17] A circular disc was loaded by two concentric rings of different diameters in the concentric-ring test. Soft interlayers between the specimen and the load and support rings reduced the frictional losses. Steel pins guaranteed the exact positioning of the rings. The load was applied via a sphere in order to minimize deviations from axisymmetry. This fixture had been used successfully in previous tests.[19] However, it is known that the soft interlayers do not completely eliminate the effect of friction, and the stresses in the disc are reduced by approximately 10% through frictional losses. This was verified by measurement of the effective stress field of the alumina specimens using strain gauges. Therefore, the experimental values of the fracture stress were multiplied by a factor of 0·9.

The cold-spin tests were performed by Daimler Benz AG in Stuttgart, Germany, and by United Turbine in Malmö, Sweden.[18] The tests were conducted in vacuum using a spin testing machine of Schenck, type BL2U. The specimens (discs with a borehole) were stuck on a mandrel and tested with a hanging spin rotor. The rotating speed was increased at a constant rate up to failure. A burst observer with a memory unit was installed in order to measure the maximum speed.

Figure 1 shows a schematic view of the Brazilian disc test in which a circular disc is subjected to

Table 2. Specimen geometries and test conditions for the various materials investigated

Test	*Geometry*	*Loading rate (MPa s^{-1})*	*Surface treatment*
Stoneware material			
Four-point bending	specimen width, B = 4·0 mm specimen thickness, H = 3·0 mm distance of specimen supports, L = 40·0 mm distance of load pins, l = 20·0 mm	60	ground, tempered at 350°C for 30 min
Concentric ring	radius of disc, R = 22·5 mm specimen thickness, t = 3·0 mm radius of support ring, r_1 = 16·0 mm radius of load ring, r_2 = 8·0 mm	15	
Brazilian disc	radius of disc, R = 22·5 mm specimen thickness, t = 7·4 mm	7	
Alumina			
Four-point bending	specimen width, B = 4·0 mm specimen thickness, H = 3·0 mm distance of specimen supports, L = 40·0 mm distance of load pins, l = 20·0 mm	450	ground, tempered at 1150°C for 5 h
Concentric ring	radius of disc, R = 22·7 mm specimen thickness, t = 3·0 mm radius of support ring, r_1 = 16·0 mm radius of load ring, r_2 = 8·0 mm	200	
Brazilian disc	radius of disc, R = 22·0 mm specimen thickness, t = 4·0 mm	5·5	
Silicon nitride (ABB and ESK materials)			
Cold-spin disc	specimen thickness, t = 10·0 mm radius of borehole, r_1 = 8·0 mm radius of disc, r_a = 51·5 mm	10	lapped and polished; no heat treatment
Brazilian disc	radius of disc, R = 22·5 mm specimen thickness, t = 4·0 mm	3	

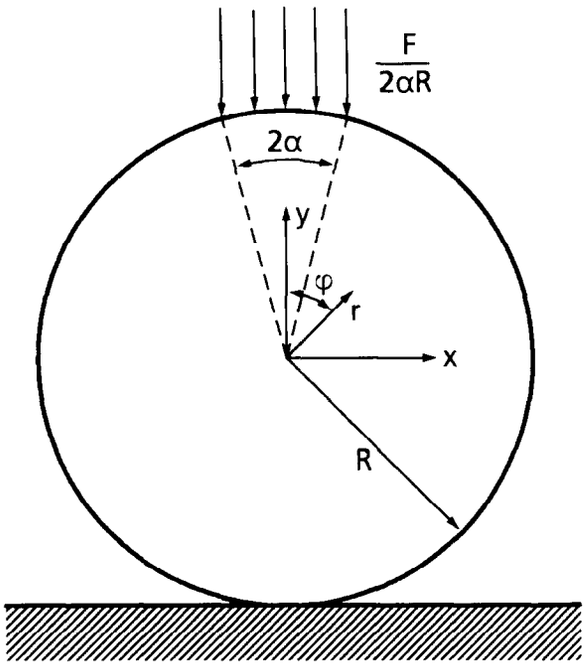

Fig. 1. Brazilian disc test.

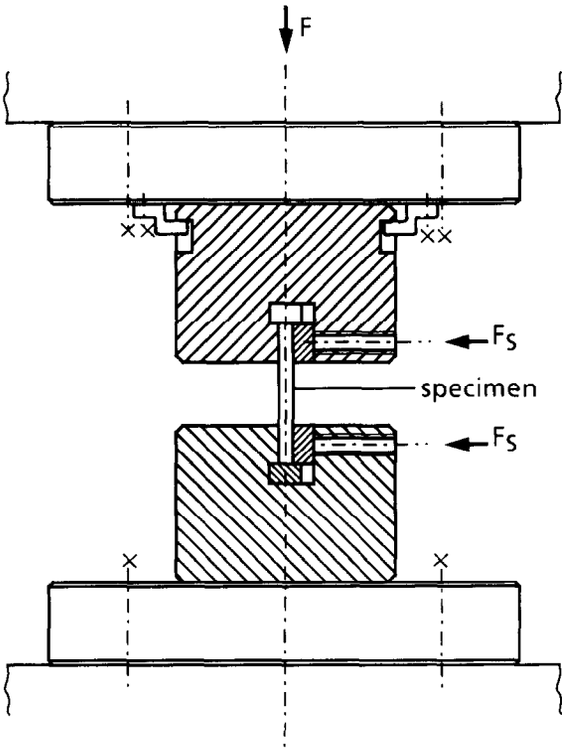

Fig. 2. Schematic view of the test rig for the Brazilian disc test.

diametral compression. Extended damage zones develop in high-strength materials due to high compressive loads in the vicinity of the load pin. Specimen failure is triggered from these zones, whereas the maximum tensile stress occurs in the centre of the disc (Ref. 10, see next section). Moreover, some specimens were split up into slices parallel to the disc surface. This failure mode starts from some point on the perimeter of

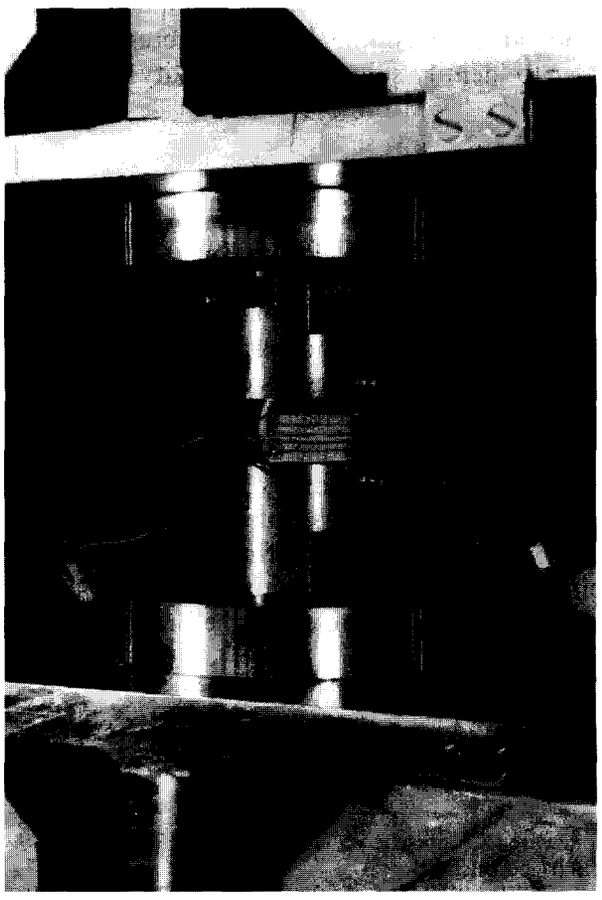

Fig. 3. Mounted specimen for the Brazilian disc test.

the disc in the vicinity of the load pin and can be attributed to stresses induced by frictional effects between the load pin and the disc.[19] A schematic view of the fixture designed for testing high-strength materials is given in Fig. 2. The load is applied via two comparatively soft steel plates which adapt to the perimeter of the specimen under load. Lateral holders are placed in the upper and lower parts of the fixture in order to keep the specimen aligned. Screws exerting the forces F_s (see Fig. 2) are fastened after a small amount of load (~100 N) has been applied. Thus, a compressive stress field is applied perpendicular to the x–y plane (see Fig. 1). After fracture, the specimens were carefully investigated. All those specimens which showed rather unusual fracture patterns were eliminated. Additionally, the location of the fracture origin was monitored by attaching to the specimen wires, interconnected by silver strips. Sequential rupture of the silver strips was recorded by a logic circuit. Figure 3 shows the specimen mounted in the fixture.

Results

Weibull analysis

The fracture stresses were calculated according to the following formulae:

four-point bend test

$$\sigma_c = \frac{3(L - l) \cdot F_c}{2BH^2} \tag{16}$$

concentric-ring test

$$\sigma_c = \frac{3(1 + \nu) \cdot F_c}{4\pi t^2}\left(2 \ln \frac{r_1}{r_2} + \frac{1 - \nu}{1 + \nu} \cdot \frac{r_1^2 - r_2^2}{R^2}\right) \tag{17}$$

cold-spin disc test

$$\sigma_c = \rho\omega_c^2 r_a^2 \frac{3 + \nu}{4} \cdot \left(1 + \frac{1 - \nu}{3 + \nu} \cdot \frac{r_i^2}{r_a^2}\right) \tag{18}$$

Brazilian disc test

$$\sigma_c = \frac{F_c}{\pi Rt} \tag{19}$$

where F_c and ω_c denote the load and the frequency at fracture, respectively, and the density is $\rho = 3{\cdot}2$ g cm^{-3} for the silicon nitride materials. The geometry variables are given in Table 2. The fracture stresses $\sigma_{c,i}$ ($i = 1, \ldots, n$, where n is the sample size of a specific test series) were ranked in ascending order and plotted on Weibull paper with the empirical probability

$$p_i = \frac{i - 0{\cdot}5}{n} \tag{20}$$

A Weibull distribution, eqn (3), was fitted to the experimental results using the maximum likelihood method.[20] A bias correction factor was introduced for the Weibull parameter m.[20] 90% confidence intervals[20] were determined in order to take into account the statistical uncertainty of the results. The results are summarized in Table 3 and in Figs 4–7. The measured values of fracture stress in the concentric-ring test were multiplied by the factor 0·9 in order to account for frictional losses. In case of the Brazilian disc, only 'valid' test results were included in the sample, i.e. the data obtained with those specimens which showed a regular fracture pattern as explained in Ref. 21 and contained at least one central crack originating outside the gripped region of the specimen.

Prediction of the failure probabilities

The failure probability for a given specimen type at a specific load level can be predicted from eqn (1), if the parameters σ_0 and m are known. In this paper eqns (14) and (15) are used, where the reference sample [index 1 in eqn (14)] is the four-point bend test in the case of the stoneware material and alumina, whereas the cold-spin-disc test is used for the silicon nitrides. The integrals over the stress fields, eqn (15), were evaluated by numerical integration. The stress fields are given by

$$\sigma_1 = \begin{cases} \sigma^* \cdot \dfrac{2}{H} \cdot y & \text{for } -\dfrac{l}{2} \le x \le \dfrac{l}{2} \\ \sigma^* \cdot \dfrac{2}{H} \cdot y \cdot \dfrac{L - 2|x|}{L - l} & \text{for } \dfrac{l}{2} < |x| \le \dfrac{L}{2} \end{cases} \tag{21}$$

Table 3. Results of the Weibull analysis for the various materials investigated

Test	*Sample size*	*Weibull parameter,* b *(MPa) [90% confidence interval]*	*Weibull parameter,* m *[90% confidence interval]*
Stoneware material			
Four-point bending	24	45·8 [45·1, 46·6]	22·5 [17·0, 29·3]
Concentric ring	17	44·0 [42·9, 45·1]	16·8 [12·1, 23·4]
Brazilian disc	20	37·5 [37·1, 37·9]	35·6 [26·4, 48·4]
Alumina			
Four-point bending	67	437 [429, 444]	12·9 [11·0, 15·1]
Concentric ring	28	379 [370, 389]	13·1 [10·2,16·9]
Brazilian disc	21	437 [424, 451]	12·6 [9·3, 17]
HIPSN (ABB material)			
Cold-spin disc	19	517 [492, 543]	8·4 [6·2, 11·5]
Brazilian disc	14	553 [529, 579]	10·5 [7·3, 15·2]
HIPSN (ESK material)			
Cold-spin disc	20	547 [518, 577]	7·3 [5·4. 9·9]
Brazilian disc	21	672 [630, 718]	6·0 [4·5, 8·2]

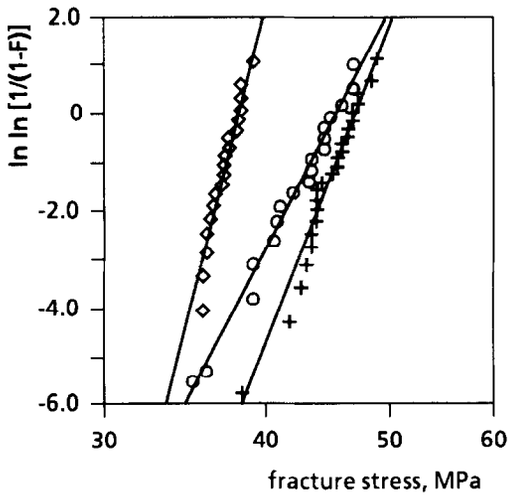

Fig. 4. Weibull plot of the test results, stoneware material. + four-point bending, ○ concentric ring, ◇ Brazilian disc.

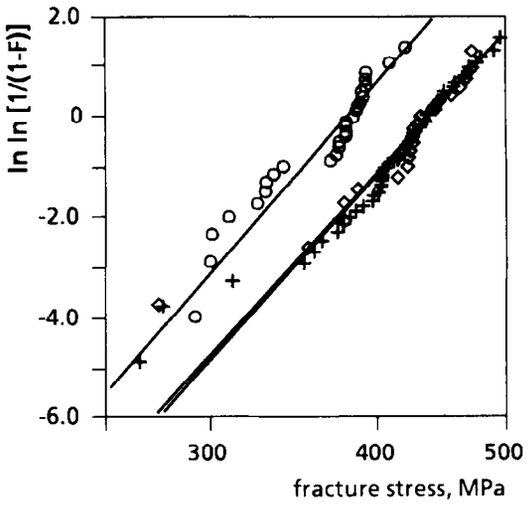

Fig. 5. Weibull plot of the test results, alumina. + four-point bending, ○ concentric ring, ◇ Brazilian disc.

for the four-point bend test with σ^* equal to σ_c in eqn (16),

$$\sigma_1 = \begin{cases} \sigma^* \cdot \dfrac{2}{t} \cdot z & \text{for } r \le r_2 \\ \dfrac{3\cdot(1+\nu)\cdot F}{4\pi t^2} \cdot \dfrac{2}{t} \cdot z \cdot \left[2\ln\dfrac{r_1}{r} + \dfrac{1-\nu}{1+\nu}\left(\dfrac{r_1^2 - r_2^2}{R^2} + \dfrac{r^2 - r_2^2}{r^2} \right) \right] & \text{for } r_2 < r \le r_1 \\ \dfrac{3\cdot(1-\nu)\cdot F}{4\pi t^2} \cdot \dfrac{2}{t} \cdot z \cdot (r_1^2 - r_2^2) \cdot \left(\dfrac{1}{R^2} + \dfrac{1}{r^2} \right) & \text{for } r_1 < r \le R \end{cases} \quad (22a)$$

for the radial stress,

$$\sigma_2 = \begin{cases} \sigma_1 & \text{for } r \le r_2 \\ \dfrac{3\cdot(1+\nu)\cdot F}{4\pi t^2} \cdot \dfrac{2}{t} \cdot z \cdot \left[2\ln\dfrac{r_1}{r} + \dfrac{1-\nu}{1+\nu}\left(\dfrac{r_1^2 - r_2^2}{R^2} + \dfrac{r^2 - r_2^2}{r^2} \right) \right] & \text{for } r_2 < r \le r_1 \\ \dfrac{3\cdot(1-\nu)\cdot F}{4\pi t^2} \cdot \dfrac{2}{t} \cdot z \cdot (r_1^2 - r_2^2) \cdot \left(\dfrac{1}{R^2} - \dfrac{1}{r^2} \right) & \text{for } r_1 < r \le R \end{cases} \quad (22b)$$

for the circumferential stress in case of the concentric-ring test with σ^* equal to σ_c in eqn (17),

$$\sigma_1 = \rho\omega^2 r_a^2 \cdot \frac{3+\nu}{8} \cdot \left(1 + \frac{r_i^2}{r_a^2} + \frac{r_i^2}{r^2} - \frac{1+3\nu}{3+\nu} \cdot \frac{r^2}{r_a^2} \right) \quad (23a)$$

for the circumferential stress,

$$\sigma_2 = \rho\omega^2 r_a^2 \cdot \frac{3+\nu}{8} \cdot \left(1 + \frac{r_i^2}{r_a^2} - \frac{r_i^2}{r^2} - \frac{r^2}{r_a^2} \right) \quad (23b)$$

for the radial stress in case of the cold-spin test, and

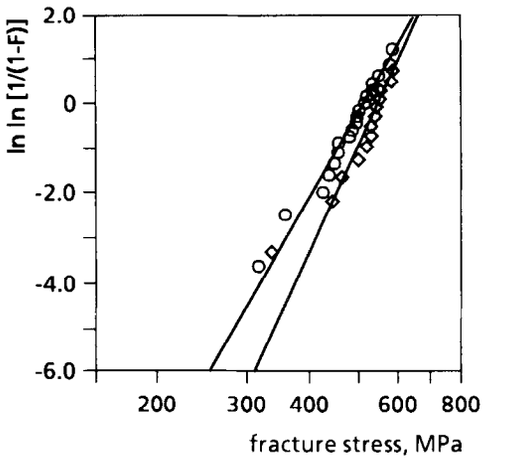

Fig. 6. Weibull plot of the test results, silicon nitride (ABB material). ○ cold spin disc, ◇ Brazilian disc.

$$\sigma_{rr} = -\sigma^* \cdot \left\{ 1 + \sum_{n=1}^{\infty} \left[1 - \left(1 - \frac{1}{n} \right) \frac{r^2}{R^2} \right] \left(\frac{r}{R} \right)^{2n-2} \cdot \frac{\sin 2n\alpha}{\alpha} \cdot \cos 2n\phi \right\} \quad (24a)$$

$$\sigma_{\phi\phi} = -\sigma^* \cdot \left\{ 1 - \sum_{n=1}^{\infty} \left[1 - \left(1 + \frac{1}{n} \right) \frac{r^2}{R^2} \right] \cdot \left(\frac{r}{R} \right)^{2n-2} \cdot \frac{\sin 2n\alpha}{\alpha} \cdot \cos 2n\phi \right\} \quad (24b)$$

$$\sigma_{r\phi} = -\sigma^* \cdot \left\{ \sum_{n=1}^{\infty} \left[1 - \left(1 + \frac{1}{n} \right) \frac{r^2}{R^2} \right] \cdot \left(\frac{r}{R} \right)^{2n-2} \cdot \frac{\sin 2n\alpha}{\alpha} \cdot \cos 2n\phi \right\} \quad (24c)$$

for the Brazilian disc, where r, ϕ and α are defined in Fig. 1.

The multiaxiality criteria, eqns (8a)–(13b), were inserted in eqns (14) and (15), and predictions of

the Weibull parameter b were obtained depending on the criterion used. The predicted value of b is considered to be compatible with the experimental values of b if the 90% confidence intervals overlap, which implies that there are common values for the estimate of the unknown parameter b. The confidence interval of the predicted value is calculated using the upper and lower bounds of the reference parameter b_1 and the bias-corrected maximum-likelihood estimate for m. The results are summarized in Table 4. According to the findings of a fractographic examination,[22] the alumina specimens contained both volume flaws and surface flaws but the surface flaws were determined to be critical. Therefore, the predictions for alumina were based on the modification of eqn (1) for surface flaws, see e.g. Ref. 8. Failure of both the stoneware and the silicon nitride materials was triggered by volume flaws.[17,22]

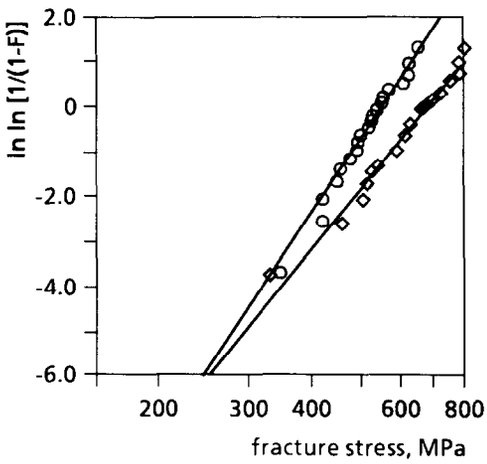

Fig. 7. Weibull plot of the test results, silicon nitride (ESK material). ○ cold spin disc, ◇ Brazilian disc.

As shown in other papers,[19,23] the difference between the predictions of the various multiaxiality criteria is very small for the concentric-ring test. Shear-sensitive criteria such as eqns (9a)–(13b) seem to be slightly superior to shear-insensitive criteria such as eqns (8a) and (8b). This is in agreement with the findings in Ref. 23, where discs containing artificial flaws were tested in diametral

Table 4.

(a) Measured and predicted values of the Weibull parameter b (in MPa), stoneware material (m = 22·5)

Test	*Concentric ring*	*Brazilian disc*
Measured value of b	[42·9, 45·1]	[37·1, 37·9]
Predicted value of b, eqns (8a), (8b)	[39·3, 40·6]	[37·8, 39·1]
Predicted value of b, eqns (9a), (9b)	[40·2, 41·5]	[9·9, 10·2]
Predicted value of b, eqns (11a), (11b)	[41·8, 43·2]	[9·6, 9·9]
Predicted value of b, eqns (12a), (12b)	[41·5, 42·9]	[10·9, 11·3]
Predicted value of b, eqns (13a), (13b)	[43·2, 44·6]	[9·5, 9·8]

(b) Measured and predicted values of the Weibull parameter b (in MPa), alumina (m = 12·9)

Test	*Double ring*	*Brazilian disc*
Measured value of b	[370, 389]	[424, 451]
Predicted value of b, eqns (8a), (8b)	[347, 458]	[438, 453]
Predicted value of b, eqns (9a), (9b)	[356, 368]	[241, 250]
Predicted value of b, eqns (11a), (11b)	[382, 395]	[217, 224]
Predicted value of b, eqns (12a), (12b)	[378, 391]	[253, 261]
Predicted value of b, eqns (13a), (13b)	[378, 391]	[216, 223]

(c) Measured and predicted values of the Weibull parameter b (in MPa) for the Brazilian disc test, HIPSN (ABB material; m = 8·4)

Measured value	[529, 579]
Predicted value, eqns (8a), (8b)	[571, 630]
Predicted value, eqns (9a), (9b)	[269, 297]
Predicted value, eqns (11a), (11b)	[258, 284]
Predicted value, eqns (12a), (12b)	[295, 326]
Predicted value, eqns (13a), (13b)	[256, 282]

(d) Measured and predicted values of the Weibull parameter b (in MPa) for the Brazilian disc test, HIPSN (ESK material; m = 7·3)

Measured value	[630, 718]
Predicted value, eqns (8a), (8b)	[636, 708]
Predicted value, eqns (9a), (9b)	[303, 338]
Predicted value, eqns (11a), (11b)	[290, 323]
Predicted value, eqns (12a), (12b)	[331, 369]
Predicted value, eqns (13a), (13b)	[287, 320]

compression. However, the results depend strongly on the effect of friction on the stress field. A slight increase in the assumed amount of frictional losses leads to a shift of the measured value of b to lower values and hence to a better agreement with the prediction based on the shear-insensitive criterion, eqn (8a) and (8b).

The Brazilian disc test, on the other hand, rules out any of the shear-sensitive criteria. Predictions and experiment agree surprisingly well with each other if eqns (8a) and (8b) are used, i.e. if it is assumed that natural flaws fail by pure mode-I fracture.

Conclusion

The Brazilian disc test is a suitable means to determine multiaxiality criteria for high-strength ceramics. The difference between the predicted failure probabilities obtained with different criteria is very large due to the stress field with both positive and negative principal stresses. The test was successfully performed for low- and high-strength ceramics using a fixture in which a compressive stress normal to the disc plane was induced by a special design of the specimen grips.

The statistical distribution of the fracture strength obtained in the Brazilian disc test can be compared with the prediction of the multiaxial Weibull theory. Based on reference tests performed with the four-point bend test or the cold-spin disc test, good agreement was only obtained if a shear-insensitive multiaxiality criterion was used.

References

1. Batdorf, S. B. & Crose, J. G., A statistical theory for the fracture of brittle structures subjected to nonuniform polyaxial stresses. *J. Appl. Mech.*, **41** (1974) 267–272.
2. Evans, A. G., A general approach for the statistical analysis of multiaxial fracture. *J. Am. Ceram. Soc.*, **61** (1978) 302–308.
3. Matsuo, Y., A probabilistic analysis of brittle fracture loci under biaxial stress state. *Bull. JSME*, **24** (1981) 290–294.
4. Paris, P. C. & Sih, G. C., Stress analysis of cracks. In ASTM STP 381, American Society for Testing and Materials, New York, 1970, pp. 30–83.
5. Erdogan, F. & Sih, G. C. On the crack extension in plates under plane loading and tranverse shear. *J. Basic Eng.*, **85** (1963) 519–527.
6. Hellen, T. K. & Blackburn, W. S., The calculation of stress intensity factors for combined tensile and shear loading. *Int. J. Fract.*, **11** (1975) 605–617.
7. Richard, H. J., Bruchvorhersagen bei überlagerter Normal- und Schubbeanspruchung von Rissen. VDI-Report No. 631/85, Düsseldorf, 1985.
8. Thiemeier, T., Brückner-Foit, A. & Kölker, H., Influence of the fracture criterion on the failure prediction of ceramics loaded in biaxial flexure. *J. Am. Ceram. Soc.*, **74** (1991) 48–52.
9. Carneiro, F. L. L. B. & Barcellos, A., Résistance à la traction des bétons. Instituto Nacional de Technologia, Rio de Janeiro, 1949.
10. Hondros, G., The evaluation of Poisson's ratio and the modulus of materials of a low tensile resistance by the Brazilian (indirect tensile) test with particular reference to concrete. *Australian J. Appl. Sci.*, **10** (1959) 243–268.
11. Mußchelishivili, G., *Einige Grundaufgaben zur mathematischen Elastizitätstheorie*. C. Hanser Verlag, München, 1971.
12. Marion, R. H. & Johnstone, J. K., A parametric study of the diametral compression test for ceramics. *Am. Ceram. Soc. Bull.*, **56** (1977) 998–1002.
13. Shaw, M. C., Braiden, P. M. & De Salvo, G. J., The disk test for brittle materials. *J. Eng. Ind.*, **97** (1975) 77–87.
14. Spriggs, R. M., Brissette, L. A. & Vasilos, T., Tensile strength of polycrystalline ceramics by the diametral compression test. *J. Mater. Res. Stand.*, **4** (1964).
15. Winter, W., Experimentelle Bestimmung der Zugfestigkeit spröder Werkstoffe (Glas, Keramik) im Scheiben-Druck-Versuch, PhD Thesis, Aachen, 1992.
16. Gumbel, E., *Statistics of Extremes*. Columbia University Press, New York, 1958.
17. DIN, Prüfung von keramischen Hochleistungswerkstoffen. DIN 51110, Part 1–3, 1990.
18. Brückner-Foit, A., Berweiler, W., Hollstein, T., Mann, A., Munz, D. & Schirmer, K.-S., Mechanical characterization of engineering ceramics. Final Report, IEA Annex II, Subtask 5, University of Karlsruhe, September 1993.
19. Schäfer, R., Soltész, U. & Bernauer, G., 3-D-Finite-Elemente-Analyse zur Lokalisierung des Bruchursprungs im Spaltzugversuch. IWM-Report W3/95, Fraunhofer-Institute for Mechanics of Materials, Freiburg, 1995.
20. Thoman, D. R., Bain, L. J. & Antle, C. E., Inferences of the parameters of the Weibull distribution. *Technometrics*, **11** (1969) 445–460.
21. Rudnick, A., Hunter, A. R. & Holden, F. C., An analysis of the diametral compression test. *Mater. Res. Stand.*, **3** (1963) 283–289.
22. Schirmer, K.-S., Entwicklung von Versagenskriterien für keramische Bauteile unter mehrachsiger Belastung. VDI-Report No. 174/95, Düsseldorf, 1995.
23. Shetty, D. K., Rosenfield, A. R. & Duckworth, W. H., Mixed-mode fracture in biaxial stress state: application of the diametral-compression test. *Eng. Fract. Mech.*, **26** (1987) 825–840.